



Green synthesis, characterization of silver nanoparticles and their study on antibacterial activity and optical limiting behavior

B. Nisha¹ · Y. Vidyalakshmi¹ · D. Geetha¹ · J. Ruhena Parveen¹ · G. Vinitha²

Received: 12 July 2018 / Accepted: 25 May 2019 / Published online: 15 June 2019
© Springer-Verlag GmbH Germany, part of Springer Nature 2019

Abstract

An enhanced method of synthesizing silver nanoparticles (AgNPs) is adopted herein using the aqueous extract of *Decalepis hamiltonii* root as both reducing and capping agents. In the recent years, metal nanoparticles have been actively synthesized using green route which is considered as an efficient, inexpensive and eco-friendly method. The generation of AgNPs was first observed from the UV–visible spectroscopy. The XRD analysis confirms the FCC structure with an average crystal size of 22 nm which is calculated using Scherrer's formula. The functional group responsible for the reduction of AgNPs is identified from the FTIR analysis. Transmission electron microscopy (TEM) showed the formation of silver nanoparticles of size ranging from 5 to 20 nm with few agglomerations. The antibacterial studies were carried out against the *Escherichia coli* and *Staphylococcus aureus* using minimum inhibitory concentration (MIC) technique. The third-order nonlinear optical properties of AgNPs were measured by the Z-scan technique. The negative nonlinearity observed was utilized for the study of optical limiting behavior.

1 Introduction

The field of nanotechnology is considered as one of the most important areas of research in the field of materials science and engineering in the twenty-first century. There has been tremendous effort to develop cost-effective and environment friendly technique for the synthesis of nanoparticles by controlling their size and shape. The applications are wide dependent on the size and shape of the nanoparticles. Recently, the importance has been placed on the synthesis of noble metal nanoparticles due to their applications in the field of electronics, optoelectronics, magnetic, information storage, catalysis, medicine, biotechnology and material sciences [1–9]. Also various plasmonic nanostructures have been used for achieving optimal localized surface plasmon resonance (LSPR) nanosensors [10, 11].

Over the last decade, noble metal nanoparticles like gold, silver, platinum, and palladium were synthesized using algae, fungi, bacteria, and plant extracts [12–16]. It is

known to be advantageous over conventional physical and chemical methods. Physical methods, such as physical vapor deposition, thermal decomposition, irradiation, etc., require maintenance of high temperature and pressure, and chemical methods involve the use of hazardous chemicals and so the biocompatibility of the resulting NPs is too low for application in biological systems. The use of plant extracts is found to be potentially advantageous over microorganisms due to the ease of improvement, the less biohazard and elaborate process of maintaining cell cultures [17]. Plant extracts are believed to act as reducing agent and stabilizing agent in the nanoparticles' synthesis. As different plant extracts contain different concentrations of biochemical reducing agents, the source of plant extract plays the most vital role in the morphology, time, and yield of the synthesized nanoparticles [18, 19].

Among the noble metal nanoparticles, silver nanoparticles have received wide attention due to their unique antibacterial, antifungal, antiviral, and anticancer activities [20–26]. Silver is an attractive material because of its unique properties such as catalytic activity, good conductivity, chemical stability and optical properties [27]. The antibacterial activity of silver nanoparticles is well known from many literatures [22–28]. The AgNPs has applications in various fields like medical, water filtration and air purification [29]. In this work, silver nanoparticles were prepared using *Decalepis*

✉ Y. Vidyalakshmi
y_vidya2003@yahoo.co.in

¹ Department of Physics, Anna University, Chennai 600025, India

² Department of Physics, VIT University, Chennai 600048, India

hamiltonii root extract and the synthesized nanoparticles were characterized by UV–visible, FTIR, XRD, and TEM analysis, and in addition, its optical limiting behavior and antibacterial activity have been studied. The *Decalepis hamiltonii* root is a medicinal plant which is useful as a blood purifier, preservative, and also as a source of bioinsecticide for stored food grains [30, 31]. The previous studies have shown that the *Decalepis hamiltonii* root extract (DHRE) contains aldehyde, inositol, saponins, amyriinsandlupeols as well as volatile compounds such as 2-hydroxy-4-methoxybenzaldehyde, vanillin, 2-phenyl ethyl alcohol, benzaldehyde and others [32, 33].

2 Experimental methods

2.1 The preparation of *Decalepis hamiltonii* root extract

Decalepis hamiltonii was purchased from local market, and cleaned thoroughly using distilled water and cut into small pieces. It was allowed to shade dry for few days and powdered. A 5 g of root powder was taken in a 100 ml beaker containing 50 ml of distilled water; the mixture was boiled at 75 °C for 30 min and then filtered using a Whatman filter paper. The filtrate was used for the synthesis of silver nanoparticles and stored in refrigerator at 4 °C for future use.

2.2 Synthesis of silver nanoparticles

About 45 ml of 1 mM AgNO₃ solution was taken in a 250 ml conical flask containing 5 ml of *D. hamiltonii* root extract. The formation of AgNPs can be seen by the color of the solution which slowly turns from light yellow to dark brown and becomes intense after 2 days is shown in Fig. 1. This is due to the surface Plasmon resonance and it was further confirmed by the UV–visible spectroscopy. The phytochemicals present in root extract slowly reduce the silver ions (Ag⁺) to form silver atoms (Ag⁰) and the efficiency of yield was found to be 80%.

3 Results and discussion

3.1 UV–visible spectroscopy

The formation of silver nanoparticles was primarily confirmed by the color change of the solution and then from the UV–visible absorption spectroscopy. DHRE is the only source that acts as both reducing and stabilizing agent. After the addition of root extract, the color of the solution turned pale yellow, but the color intensified after few days, and finally, it reached dark brown color which indicates the



Fig. 1 Color change of the synthesized silver nanoparticles

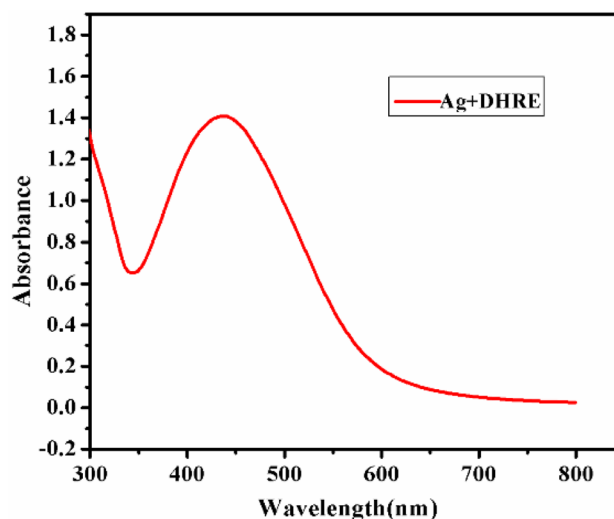


Fig. 2 UV–visible absorbance spectra of silver nanoparticles

reduction of AgNPs. UV–visible absorption spectra shown in Fig. 2 clearly predict the absorption peak which arises due to the surface plasmon excitation [34]. A well-defined broad absorption peak around 436 nm was observed which may be due to poly-dispersed nanoparticles [35, 36].

3.2 X-ray diffraction studies

The X-ray diffraction pattern for the prepared silver nanoparticles is shown in Fig. 3. The XRD analysis shows that the synthesized AgNPs are crystalline in nature. The 2θ values were taken from 20° to 70° and the Bragg reflections were observed at 38, 44.2, and 64.2 which correspond to the indexed planes of crystals of Ag (111), (200), and (220). The average crystallite size was found to be 22.4 nm,

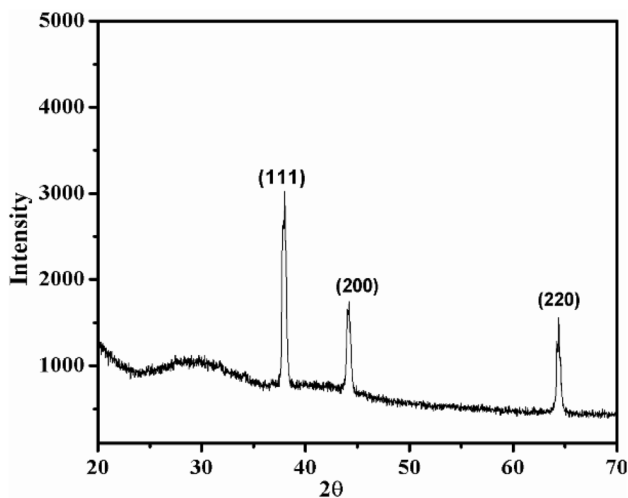


Fig. 3 XRD pattern of silver nanoparticles

calculated from the Scherrer formula, and it exhibits cubic face-centered structure with space group $fm\bar{3}m$. The cell parameter was found to be in good agreement with the database of JCPDS Card no. 04-0783 [36, 37].

3.3 Fourier transform infrared spectroscopy analysis

FTIR studies were undergone to identify the presence of biomolecules responsible for the synthesis of AgNPs. The FTIR analysis of AgNPs is shown in Fig. 4. The absorption is observed at different wave numbers indicating the biomolecules responsible for the reduction of AgNPs. The peaks appeared at 1025 and 3398 are referred as the strong bands. The band at 1025 assigned as absorption peaks of C–O–C– [38]. The absorption peak at 3398 indicates the N–H stretching. The absorption band present at 1378 corresponds to N=O symmetric stretching. The peaks at 2924 cm^{-1} give the aldehydic C–H stretching. The medium absorption band at 1637 is due to the C–N and C–C stretching which proves the presence of proteins [39, 40].

3.4 Transmission electron microscopy analysis

The transmission electron microscopy (TEM) analysis is carried out using the instrument JEOL JEM 2100. TEM study clearly predicts the size, shape and morphology of the silver nanoparticles. Figure 5 represents the

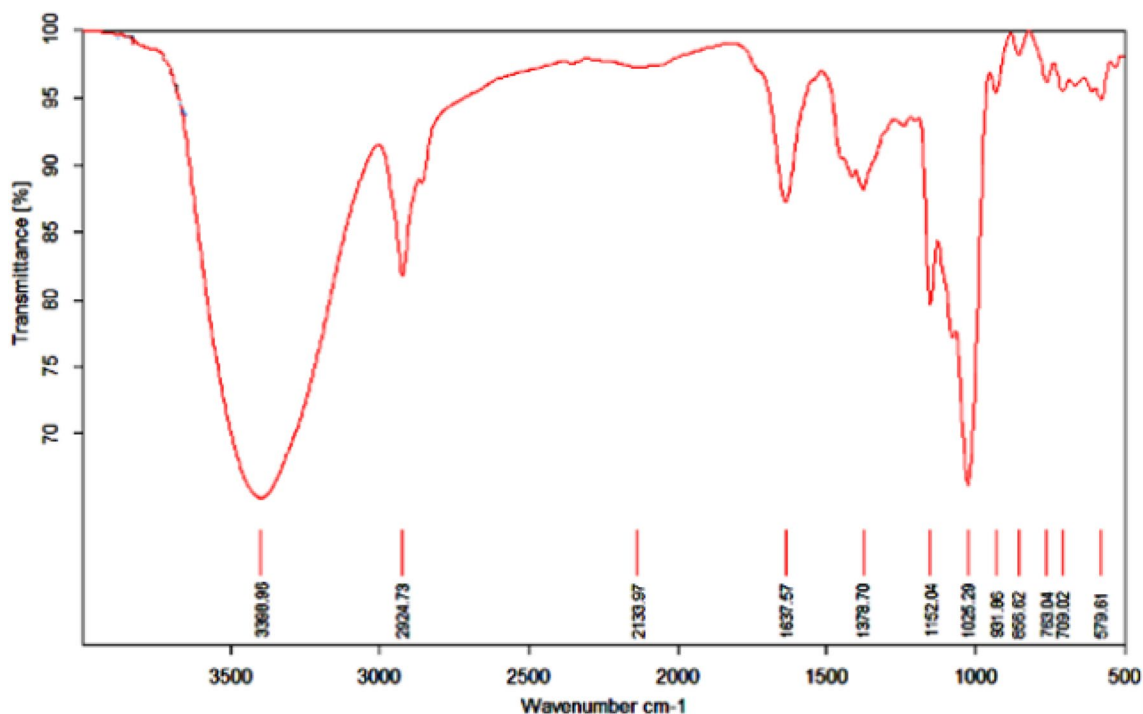
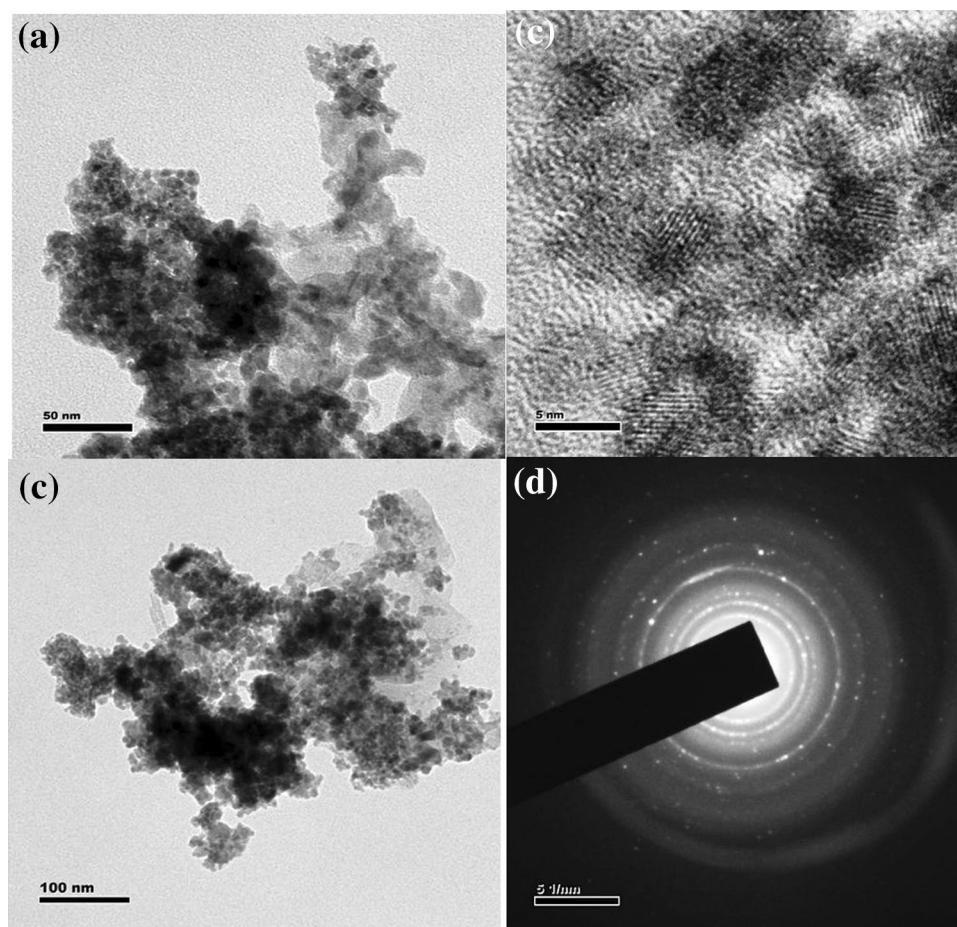


Fig. 4 FTIR spectra of AgNPs

Fig. 5 TEM image of AgNPs: **a** 50 nm, **b** 5 nm, **c** 100 nm, and **d** SAED pattern of AgNPs



TEM image of the silver nanoparticles. From the figure, spherical-shaped silver nanoparticles of size ranging from 5 to 20 nm with slight agglomeration are observed. The SAED pattern proves that the particle is in circular ring like pattern which is shown in Fig. 5d. It confirms the crystalline nature of the prepared nanoparticles and the d spacing value is calculated to be 0.229 nm. Figure 6 shows

the energy-dispersive X-ray analysis (EDAX) spectrum of synthesized silver nanoparticles. The present investigation of synthesized silver nanoparticles shows strong absorption peak in the range 2.5–3.0 keV. Earlier studies have reported that the formation of silver nanoparticles was in the range 2.5–3.5 keV [41].

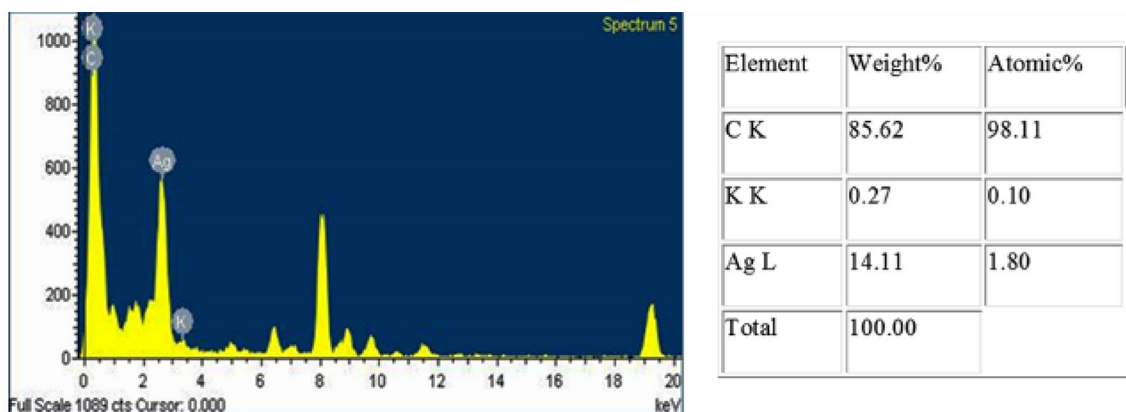


Fig. 6 EDAX pattern of AgNPs

3.5 Antibacterial studies

The minimum inhibitory concentration (MIC) describes that the lowest concentration of materials inhibits the growth of an organism which was evaluated based on batch cultures containing varying concentration (100%, 50%, 25%, 12.5%, 6.2%, 3.1%, and 1.5%) of AgNPs in suspensions. Minimum bactericidal concentration (MBC) which reports the lowest concentration of nanoparticles that inhibits 99.9% of the bacteria was also determined from the batch culture studies. To one row, each well received 100 μ l of *S. aureus* culture and to the other row culture of *E. coli* was added. The plate was incubated for 24 h and the growth of organisms was noted to obtain MIC. Subcultures were made from these wells on to NA plates and the plates incubated for 24–48 h to get the colony growth. The growth was noted to get the MBC. The Gram-positive bacteria and Gram-negative *E. coli* were grown in culture tube and it was sealed tightly. AgNPs solution was added in the grown culture tubes. From the results, it was observed that there was a zone inhibition at two different concentrations, i.e., at 50% and 100% concentrations. Furthermore, it was also found that the inhibition zone is more in Gram-negative *E. coli* than Gram-positive *S. aureus*. This may be due to the membrane thickness [42, 43]. This result confirms that silver nanoparticles have good bactericidal effect. The minimum bactericidal concentration is 100% of the original solution for *S. aureus* and 50% of the original solution for *E. coli*, respectively (Fig. 7).

3.6 Nonlinear optical studies (z-scan)

Nonlinear optical (NLO) materials play a major role in the technology and research areas because of their potential applications in various fields such as new frequency generation, different wavelength laser from the same source, information processing, optical computing, telecommunication [44–47], and optical power limiting [48]. The nonlinear optical property was studied by Z-scan technique developed by Sheik-Bahae et al. [49]. In this technique, the intensity varies along the axis of the convex lens and is maximum at the focus. This technique is highly sensitive and useful tool for determining the sign and magnitude of nonlinear refractive index (n_2) from the closed aperture and nonlinear absorption coefficient (β) from the open aperture. The colloidal silver nanoparticles have been subjected to nonlinear optical studies using 532 nm Nd:YAG (CW) laser beam. The sample was mounted on a translation stage and moved across the focal region (+ z to - z) along the direction of propagation of the laser beam and the corresponding normalized transmission was measured with and without aperture in the far field of the lens as the samples moved through the focal point.

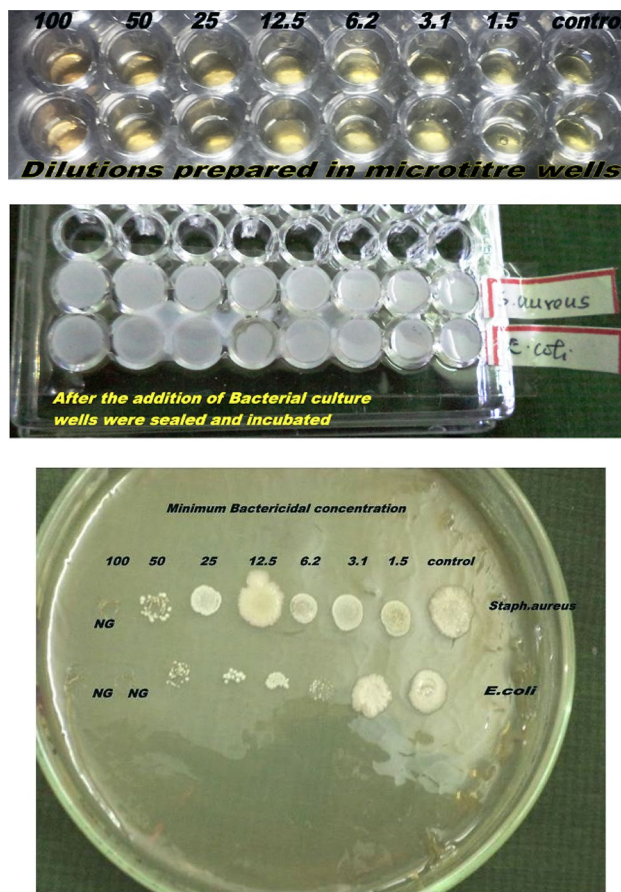


Fig. 7 Antibacterial study of AgNPs

The transmission difference between peak and valley, linear transmittance aperture, the third-order nonlinear refractive index (n_2) of the crystal, the nonlinear absorption coefficient (β), and the third-order nonlinear optical susceptibility (χ^3) were determined as the procedure given in the literature [50]. The real part $\text{Re}(\chi^3)$ is proportional to the nonlinear refractive index of the nanoparticles, while the imaginary part $\text{Im}(\chi^3)$ is proportional to the nonlinear absorption coefficient (β).

The closed aperture and open aperture Z-scan curves are illustrated in Fig. 8a, b. In the closed Z-scan curve, there is a peak followed by a valley and it corresponds to the signature of negative nonlinearity. Figure 8c gives the ratio of closed-to-open aperture scan.

The measurable quantity ΔT_{p-v} can be defined as the difference between the normalized peak and valley transmittances, $T_p - T_v$. The variation of this quantity as a function of $|\Delta\phi_0|$ is given by the following:

$$\Delta T_{p-v} = 0.406(1 - S)^{0.25} |\Delta\phi_0|, \quad (1)$$

where $\Delta\phi_0$ is the on-axis phase shift at the focus. S , the aperture linear transmittance, is given by

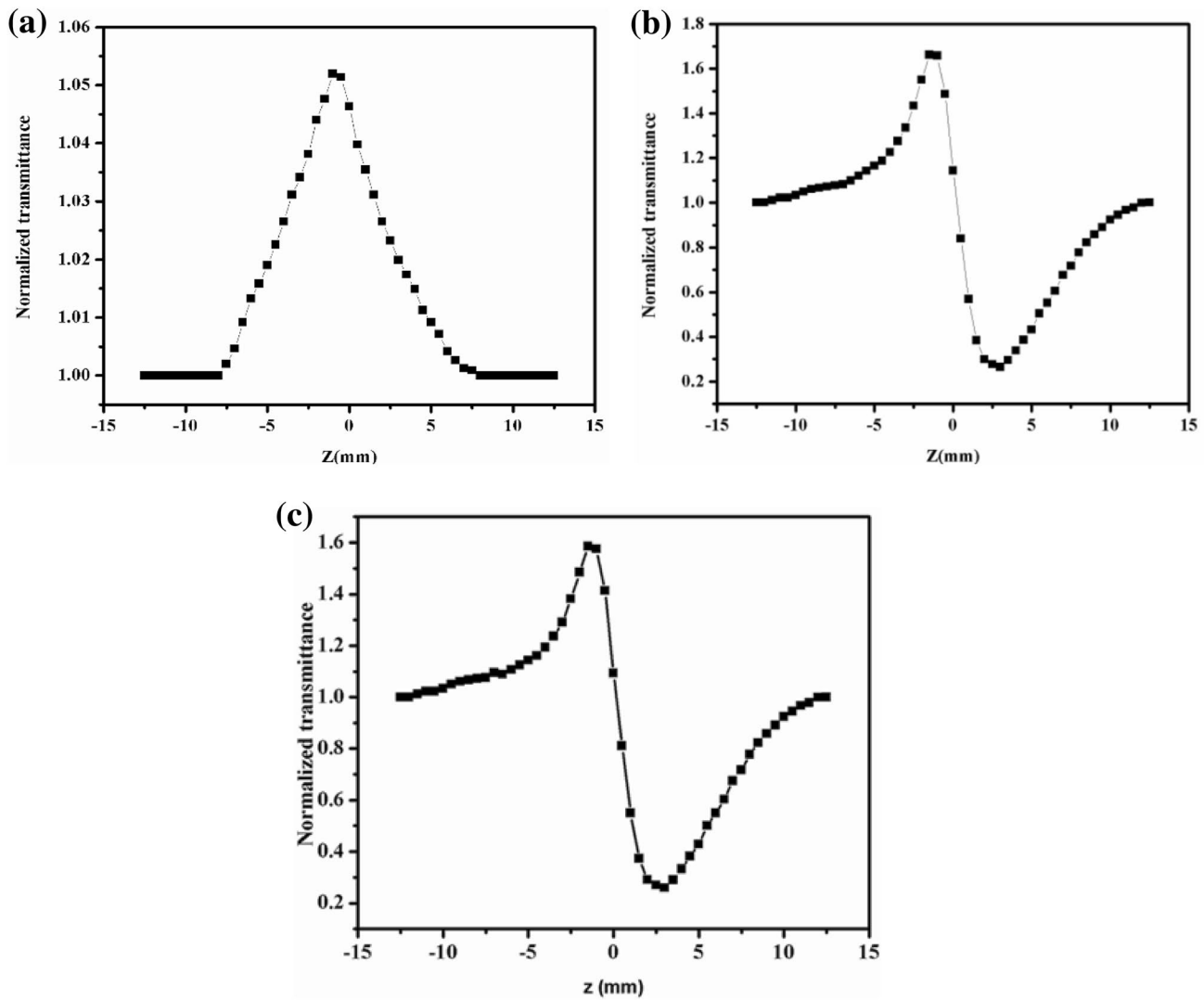


Fig. 8 **a** Z-scan open aperture curve for AgNPs. **b** Z-scan closed aperture for the prepared. **c** Ratio of closed-to-open aperture

$$S = 1 - \exp(-2r_a^2 a / \omega_a^2), \tag{2}$$

with r_a denoting the aperture radius and ω_a denoting the radius of the laser spot before the aperture.

The on-axis phase shift is related to the third-order nonlinear refractive index (n_2) by the following:

$$|\Delta\phi_0| = kn_2 L_{\text{eff}} I_0, \tag{3}$$

where $L_{\text{eff}} = (1 - e^{-\alpha L}) / \alpha$, with L the sample length, α is the linear absorption coefficient, I_0 is the intensity of the laser beam at focus $z=0$, and k is the wave number ($k=2\pi/\lambda$)

The imaginary parts of the third-order nonlinear optical susceptibility [χ^3] are estimated using the value of the nonlinear absorption coefficient β obtained from the open aperture Z-scan data and using the relations:

$$q_o(z) = \frac{\beta \times I_0 \times L_{\text{eff}}}{\left(1 + \frac{z^2}{Z_0^2}\right)} \tag{4}$$

$$\beta = \frac{2\sqrt{2} \times \Delta T}{I_0 \times L_{\text{eff}}}, \tag{5}$$

$Z_R = k\omega_0^2/2$ is the diffraction length of the beam and ω_0 is the beam waist radius at the focal point.

Experimentally determined nonlinear refractive index n_2 and nonlinear absorption coefficient β can be used in finding the real and imaginary parts of the third-order nonlinear optical susceptibility [χ^3] according to the following relations:

$$\text{Re}\chi^3 \text{ (esu)} = 10^{-4} \frac{\epsilon_0 c^2 n_0^2}{\pi} n_2 \text{ (cm}^2/\text{W)}, \tag{6}$$

$$\text{Im}\chi^3 \text{ (esu)} = 10^{-2} \frac{\epsilon_0 c^2 n_0^2 \lambda}{4\pi^2} \beta \text{ (cm/W)}, \tag{7}$$

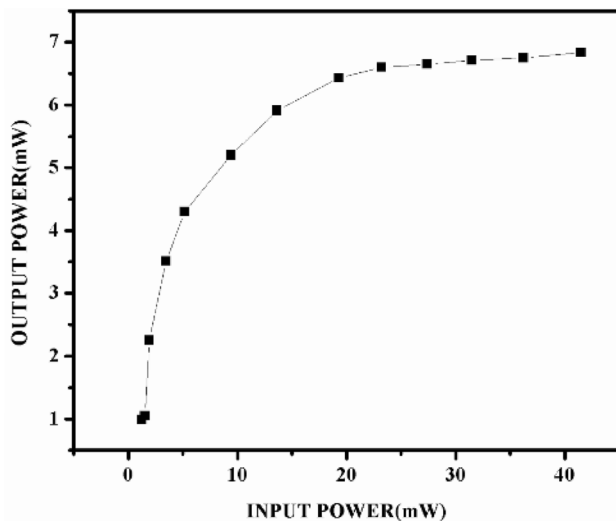


Fig. 9 Optical limiting profile for the prepared silver nanoparticles

where ϵ_0 is the vacuum permittivity and c is the light velocity in vacuum.

The absolute value of the third-order nonlinear optical susceptibility [51] is given by the relation:

$$|\chi^3| = [(\text{Re}(\chi^3))^2 + (\text{Im}(\chi^3))^2]^{1/2}. \quad (8)$$

The calculated value of the nonlinear refractive index n_2 is $7.15 \times 10^{-8} \text{ cm}^2/\text{W}$. The value of nonlinear absorption coefficient (β) estimated from the open aperture Z-scan curve is $0.04 \times 10^{-4} \text{ cm/W}$ and the third-order susceptibility (χ^3) is $4.30 \times 10^{-6} \text{ esu}$.

In optical limiting, the negative nonlinear property of silver nanoparticles is utilized, and in this process, the transmittance of a material remains constant with increase in incident light intensity. Figure 9 shows the optical limiting behavior in which transmitted output power is found to vary linearly with the incident input power. With further increase of input power, the transmitted power reaches saturation at a point defined as the limiting amplitude, i.e., the maximum output intensity. This shows that silver nanoparticles have good optical limiting property. These materials protect human eye and optical sensors from intense radiation fields [52].

4 Conclusion

In essence, synthesis of AgNPs using *D. hamiltonii* root extract by eco-friendly, non toxic and inexpensive green method is presented here. The as-synthesized nanoparticles show good stability for a period of more than 3 months at room temperature. The synthesized nanoparticles were

characterized using UV-visible, XRD, FTIR, and TEM spectroscopic techniques. Using Z-scan techniques, the nonlinear refraction and absorption coefficient were measured. The nonlinear refractive index n_2 is found to be $7.15 \times 10^{-8} \text{ cm}^2/\text{W}$, the nonlinear absorption coefficient (β) is $0.04 \times 10^{-4} \text{ cm/W}$, and the third-order nonlinear susceptibility (χ^3) is obtained as $4.30 \times 10^{-6} \text{ esu}$. Efficient antibacterial activity was also proved by the synthesized AgNPs. From the present investigation, we conclude that the optical nonlinearity of silver nanoparticles is comparable or superior to those synthesized through other methods.

Compliance with ethical standards

Conflict of interest On behalf of all authors, the corresponding author states that there is no conflict of interest.

References

1. S. Sunkar, C.V. Nachiyar, Biogenesis of antibacterial silver nanoparticles using the endophytic bacterium *Bacillus cereus* isolated from *Garcinia xanthochymus*. Asian Pac. J. Trop. Biomed. **2**, 953–959 (2012). [https://doi.org/10.1016/S2221-1691\(13\)60006-4](https://doi.org/10.1016/S2221-1691(13)60006-4)
2. S.J. Park, S.W. Lee, K.J. Lee, J.H. Lee, K.D. Kim, J.H. Jeong, J.H. Choi, An Antireflective nanostructure array fabricated by nanosilver colloidal lithography on a silicon substrate. Nanoscale Res. Lett. **5**, 1570–1577 (2010). <https://doi.org/10.1007/s11671-010-9678-y>
3. W. Li, S. Seal, E. Megan, J. Ramsdell, K. Scammon, L. Lelong, L. Lachal, K.A. Richardson, Physical and optical properties of sol-gel nano-silver doped silica film on glass substrate as a function of heat-treatment temperature. J. Appl. Phys. **93**, 9553–9561 (2003). <https://doi.org/10.1063/1.1571215>
4. V.I. Pârăulescu, B. Cojocaru, V. Pârăulescu, R. Richards, Z. Li, C. Cadigan, P. Granger, P. Miquel, C. Hardacre, Sol-gel-entrapped nano silver catalysts-correlation between active silver species and catalytic behavior. J. Catal. **25**, 92–100 (2010). <https://doi.org/10.1016/j.jcat.2010.03.008>
5. V.K. Shukla, R.S. Yadav, P. Yadav, A.C.J. Pandey, Green synthesis of nanosilver as a sensor for detection of hydrogen peroxide in water. J. Hazard. Mater. **2012**, 161–166 (2012). <https://doi.org/10.1016/j.jhazmat.2012.01.071>
6. M. Gratzel, Photoelectrochemical cells. Nature **414**, 338–344 (2001). <https://doi.org/10.1038/35104607>
7. M. Okuda, Y. Kobayashi, K. Suzuki, K. Sonoda, T. Kondoh, A. Wagawa, A. Kondo, H. Yoshimura, Self-organized inorganic nanoparticle arrays on protein lattices. Nano Lett. **5**, 991–993 (2005). <https://doi.org/10.1021/nl050556q>
8. J. Dai, M.L. Bruening, Catalytic nanoparticles formed by reduction of metal ions in multilayered polyelectrolyte films. Nano Lett. **2**, 497–501 (2005). <https://doi.org/10.1021/nl025547>
9. C.B. Murray, S. Sun, H. Doyle, T. Betley, Monodisperse 3d transition metal (Co, Ni, Fe) nanoparticles. MRS Bull. **26**, 985–991 (2001). <https://doi.org/10.1557/mrs2001.254>
10. Matthew E. Stewart, Christopher R. Anderton, Lucas B. Thompson, Joana Maria, Stephen K. Gray, John A. Rogers, Ralph G. Nuzzo, Nanostructured plasmonic sensors. Chem. Rev. **108**, 494–521 (2008)

11. T. Chung, S.-Y. Lee, E.Y. Song, H. Chun, B. Lee, Plasmonic nanostructures for nano-scale bio-sensing. *Sensors* **11**, 10907–10929 (2011). <https://doi.org/10.3390/s111110907>
12. S.P. Dubey, M. Lahtinen, M. Sillanpää, Tansy fruit mediated greener synthesis of silver and gold nanoparticles. *Process Biochem.* **45**, 1065–1071 (2010). <https://doi.org/10.1016/j.procbio.2010.03.024>
13. J. Kasthuri, K. Kathiravan, N. Rajendiran, Phyllanthin-assisted biosynthesis of silver and gold nanoparticles: a novel biological approach. *J. Nanopart. Res.* **11**, 1075–1085 (2009). <https://doi.org/10.1007/s11051-008-9494-9>
14. R.N. Rati, P. Nilotpala, B. Debadhyan, M.P. Kshyama, M. Srabani, B.S. Lala, K.M. Barada, Green synthesis of silver nanoparticle by *Penicillium purpurogenum* NPMF: the process and optimization. *J. Nanopart. Res.* **13**, 3129–3137 (2011). <https://doi.org/10.1007/s11051-010-0208-8>
15. S.R. Boddu, V.R. Gutti, T.K. Ghosh, R.V. Tompson, S.K. Loyalka, Gold silver and palladium nanoparticles/nanoagglomerate generation, collection, and characterization. *J. Nanopart. Res.* **13**, 6591–6601 (2011). <https://doi.org/10.1007/s11051-011-0566-x>
16. D.S. Shenoy, D. Philip, J. Mathew, Rapid green synthesis of palladium nanoparticles using the dried leaf of *Anacardium occidentale*. *Spectrochim. Acta A Mol. Biomol. Spectrosc.* **91**, 35–38 (2012). <https://doi.org/10.1016/j.saa.2012.01.063>
17. K. Kalishwaralal, V. Deepak, S. Ram Kumar Pandian, M. Kottaisamy, S. Barathmani Kanth, B. Kartikeyan, S. Gurunathan, Biosynthesis of silver and gold nanoparticles using *Brevibacterium casei*. *Colloids Surf B Biointerfaces* **77**, 257–262 (2010). <https://doi.org/10.1016/j.colsurfb.2010.02.007>
18. K. Mukunthan, S. Balaji, Cashew apple juice (*Anacardium occidentale* L.) speeds up the synthesis of silver nanoparticles. *Int. J. Green. Nanotechnol.* **4**(2), 71–79 (2012). <https://doi.org/10.1080/19430892.2012.676900>
19. X. Li, H. Xu, Z.S. Chen, G. Chen, Biosynthesis of nanoparticles by microorganisms and their applications. *J. Nanomater.* (2011). <https://doi.org/10.1155/2011/270974>. (Article ID 270974)
20. A.R. Shahverdi, A. Fakhimi, H.R. Shahverdi, S. Minaian, Synthesis and effect of silver nanoparticles on the antibacterial activity of different antibiotics against *Staphylococcus aureus* and *Escherichia coli*. *Nanomedicine* **3**(2), 168–171 (2007). <https://doi.org/10.1016/j.nano.2007.02.001>
21. S.S. Khan, A. Mukherjee, N. Chandrasekaran, Studies on interaction of colloidal silver nanoparticles (SNPs) with five different bacterial species. *Colloids Surf. B* **87**(1), 129–138 (2011). <https://doi.org/10.1016/j.colsurfb.2011.05.012>
22. F. Martinez-Gutierrez, P.L. Olive, A. Banuelos, E. Orrantia, N. Nino, E.M. Sanchez, F. Ruiz, H. Bach, Y. Av-Gay, Synthesis, characterization, and evaluation of antimicrobial and cytotoxic effect of silver and titanium nanoparticles. *Nanomedicine* **6**(5), 681–688 (2010). <https://doi.org/10.1016/j.nano.2010.02.001>
23. T. Premkumar, Y. Lee, K.E. Geckeler, Macrocycles as a tool: a facile and one-pot synthesis of silver nanoparticles using cucurbituril designed for cancer therapeutics. *Chem. Eur. J.* **16**(38), 11563–11566 (2010). <https://doi.org/10.1002/chem.201001325>
24. H.H. Lara, N.V. Ayala-Nuñez, L. Ixtepan-Turrent, C. Rodriguez-Padilla, Mode of antiviral action of silver nanoparticles against HIV-1. *J. Nanobiotechnol.* **8**, 1 (2010). <https://doi.org/10.1186/1477-3155-8-1>
25. D.R. Monteiro, S. Silva, M. Negri, L.F. Gorup, E.R. de Camargo, R. Oliveira, D.B. Barbosa, M. Henriques, Silver nanoparticles: influence of stabilizing agent and diameter on antifungal activity against *Candida albicans* and *Candida glabrata* biofilms. *Lett. Appl. Microbiol.* **54**(5), 383–391 (2012). <https://doi.org/10.1111/j.1472-765X.2012.03219.x>
26. A. Panáček, M. Kolár, R. Vecerová, R. Prucek, J. Soukupová, V. Krystof, P. Hamal, R. Zboril, L. Kvítek, Antifungal activity of silver nanoparticles against *Candida* spp. *Biomaterials* **30**(31), 6333–6340 (2009). <https://doi.org/10.1016/j.biomaterials.2009.07.065>
27. Y. Sun, B.T. Mayers, Y. Xia, Template-engaged replacement reaction: a one-step approach to the large-scale synthesis of metal nanostructures with hollow interiors. *Nano Lett.* **2**, 481–485 (2002). <https://doi.org/10.1021/nl025531v>
28. L. Stephan, A.E. Mostafa, Spectral properties and relaxation dynamics of surface plasmon electronic oscillations in gold and silver nanodots and nanorods. *J. Phys. Chem. B* **103**(40), 8410–8426 (1999). <https://doi.org/10.1021/jp9917648>
29. A. Frattini, N. Pellegrini, D. Nicastro, O. de Sanctis, Effect of amine groups in the synthesis of Ag nanoparticles using aminosilanes. *Mater. Chem. Phys.* **94**(1), 148–152 (2005). <https://doi.org/10.1016/j.matchemphys.2005.04.023>
30. J. George, J. Pereira, S. Divakar, K. Udaysankar, G.A. Ravi Shankar: A method for the preparation of active fraction from the root of *Decalepis hamiltonii*; useful as bio insecticide. 1998. Indian Patent No. 1301/Dec/98
31. J. George, J. Pereria, S. Divakar, K. Udaysankar, G.A. Ravishankar, Bioinsecticide from swallow root (*Decalepis hamiltonii*) wight and protects food grains against insect infestation. *Curr. Sci.* **77**, 501–502 (1999)
32. T.S. Muralidhar, S. Acharya, C. Ramyashree, S. Reddy, M.R. Shruthi, S.S. Lingaiah, Study of bioactive components in *Decalepis hamiltonii* in vitro. *IOSR J. Pharm.* **4**, 62–66 (2014)
33. P. Prakash, G. Thiyagarajan, R. Manivasagaperumal, Phytochemical screening and antibacterial activity of root extracts of *Decalepis hamiltonii* Wight & Arn. *Int J Pharma Res Rev.* **3**(11), 33–38 (2014). (ISSN: 2278-6074)
34. P. Mulvaney, Surface plasmon spectroscopy of nanosized metal particles. *Langmuir* **12**(3), 788–800 (1996). <https://doi.org/10.1021/la9502711>
35. H.M.M. Ibrahim, Green synthesis and characterization of silver nanoparticles using banana peel extract and their antimicrobial activity against representative microorganisms. *J. Radiat. Res. Appl. Sci.* **1**, 1 (2015). <https://doi.org/10.1016/j.jrras.2015.01.007>
36. Daizy Philip, Honey mediated green synthesis of silver nanoparticles. *Spectrochim. Acta Part. A* **75**(3), 1078–1081 (2010). <https://doi.org/10.1016/j.saa.2009.12.058>
37. V. Kathiravan, S. Ravi, S. Ashokkumar, Synthesis of silver nanoparticles from *Melia dubia* leaf extract and their in vitro anticancer activity. *Spectrochim. Acta A Mol. Biomol. Spectrosc.* **130**, 116–121 (2014). <https://doi.org/10.1016/j.saa.2014.03.107>
38. D. Philip, C. Unni, Extracellular biosynthesis of gold and silver nanoparticles using *Krishna tulsi* (*Ocimum sanctum*) leaf. *Phys. E* **43**(7), 1318–1322 (2011). <https://doi.org/10.1016/j.physe.2010.10.006>
39. P. Prakash, P. Gnanaprakasam, R. Emmanuel, S. Arokiyaraj, M. Saravanan, Green synthesis of silver nanoparticles from leaf extract of *Mimusops elengi*, Linn. For enhanced antibacterial activity against multi drug resistant clinical isolates. *Colloids Surf. B Biointerfaces* **108**, 255–259 (2013). <https://doi.org/10.1016/j.colsurfb.2013.03.017>
40. K. Jyoti, M. Baunthiyal, A. Singh, Characterization of silver nanoparticles synthesized using *Urtica dioica* Linn. leaves and their synergistic effects with antibiotics. *J. Radiat. Res. Appl. Sci.* **9**, 217–227 (2016)
41. S. Palanisamy, P. Rajasekar, G. Vijayaprasath, G. Ravi, R. Manikandan, N.M. Prabhu, A green route to synthesis silver nanoparticles using *Sargassum polycystum* and its antioxidant and cytotoxic effects: an in vitro analysis. *Mat Lett.* **189**, 196–200 (2017)
42. S. Prabhu, E.K. Poulouse, Silver nanoparticles: mechanism of antimicrobial action, synthesis, medical applications, and toxic effects. *Int. Nano Lett.* **2**, 32 (2012)

43. J.S. Kim, E. Kuk, K.N. Yu, J.H. Kim, S.J. Park, H.J. Lee, S.H. Kim, Y.K. Park, Y.H. Park, C.Y. Hwang, Y.K. Kim, Y.S. Lee, D.H. Jeong, M.H. Cho, Antimicrobial effects of silver nanoparticles. *Nanomed. Nanotechnol. Biol. Med.* **3**, 95–101 (2007)
44. M. Spasenovi, M. Betz, L. Costa, H.M. Van Driel, All-optical coherent control of electrical currents in centrosymmetric semiconductors. *Phys. Rev.* **77**, 085201 (2008)
45. D.S. Chemla, J. Zyss, *Nonlinear Optical Properties of Organic Molecules and Crystals*, vol. 1 (Academic Press, London, 1987)
46. J. Zyss, *Molecular Nonlinear Optics: Materials Physics and Devices* (Academic Press, New York, 1993)
47. J. Badan, R. Hierle, A. Perigand, J. Zyss, in *Nonlinear Optical Properties of Organic Molecules and Polymeric Materials*, vol. 233 D. 5, ed. by D.J. Williams (American Chemical Society, Washington, DC, 1993)
48. C.Q. Tang, Q. Zheng, H.M. Zhu, L.X. Wang, S.C. Chen, E. Ma, X.Y. Chen, Two-photon absorption and optical power limiting properties of ladder-type tetraphenylene cored chromophores with different terminal groups. *J. Mater. Chem. C* **1**, 1771–1780 (2013)
49. M. Sheik-Bahae, A.A. Said, T.H. Wei, D.J. Hagan, E.W. Van Stryland, Sensitive measurement of optical nonlinearities using a single beam. *IEEE J. Quantum Electron.* **26**, 760–769 (1990)
50. A. Shanthi, C. Krishnan, P. Selvarajan, Growth and characterization of a single crystal of urea adipic acid (UAA)—a third order nonlinear optical material. *Spectrochim. Acta A Mol. Biomol. Spectrosc.* **122**, 521–528 (2014)
51. Shalini P. Delphia, S. Senthil, P. Kannan, G. Vinitha, A. Ramalingam, Investigation on substituent effect in novel azo-naphthol dyes containing polymethacrylates for non-linear optical studies. *J. Phys. Chem. Solids* **68**, 1812–1820 (2007)
52. M. Hanack, T. Schneider, M. Barthel, J.S. Shirk, S.R. Flom, R.G.S. Pong, Indium phthalocyanines and naphthalocyanines for optical limiting. *Coord. Chem. Rev.* **219**, 235–258 (2001). [https://doi.org/10.1016/S0010-8545\(01\)00327-7](https://doi.org/10.1016/S0010-8545(01)00327-7)

Publisher's Note Springer Nature remains neutral with regard to jurisdictional claims in published maps and institutional affiliations.